AFRL-ML-WP-TP-2004-400

COARSENING BEHAVIOR OF AN ALPHA-BETA TITANIUM ALLOY

S.L. Semiatin

Metals Branch (AFRL/MLLM)
Metals, Ceramics, and Nondestructive Evaluation Division
Materials and Manufacturing Directorate
Air Force Research Laboratory, Air Force Materiel Command
Wright-Patterson AFB, OH 45433-7750

B.C. Kirby
Wright State University

G.A. Salishchev
Institute for Metals Superplasticity Problems

NOVEMBER 2004

Approved for public release; distribution is unlimited.

STINFO FINAL REPORT

MATERIALS AND MANUFACTURING DIRECTORATE
AIR FORCE RESEARCH LABORATORY
AIR FORCE MATERIEL COMMAND
WRIGHT-PATTERSON AIR FORCE BASE, OH 45433-7750

NOTICE

Using government drawings, specifications, or other data included in this document for any purpose other than government procurement does not in any way obligate the U.S. Government. The fact that the government formulated or supplied the drawings, specifications, or other data does not license the holder or any other person or corporation; or convey any rights or permission to manufacture, use, or sell any patented invention that may relate to them.

This report has been reviewed by the AFRL Wright Site Office of Public Affairs (WS/PA) and is releasable to the National Technical Information Service (NTIS). At NTIS, it will be available to the general public, including foreign nationals.

This technical report has been reviewed and is approved for publication.

//s//

Pamela M. Schaefer
Principal Materials Engineer
Technical & Strategic Planning Office
Materials and Manufacturing Directorate

Copies of this report should not be returned unless return is required by security considerations, contractual obligations, or notice on a specific document.

REPORT DOCUMENTATION PAGE

Form Approved
OMB No. 0704-0188

1. REPORT DATE *(DD-MM-YY)*	2. REPORT TYPE	3. DATES COVERED *(From - To)*
November 2004	Conference paper preprint	

4. TITLE AND SUBTITLE
COARSENING BEHAVIOR OF AN ALPHA-BETA TITANIUM ALLOY

5a. CONTRACT NUMBER
IN-HOUSE

5b. GRANT NUMBER

5c. PROGRAM ELEMENT NUMBER
N/A

6. AUTHOR(S)
S. L. Semiatin (Metals Branch (AFRL/MLLM), Metals, Ceramics, and Nondestructive Evaluation Division)
B. C. Kirby (Wright State University)
G. A. Salishchev (Institute for Metals Superplasticity Problems)

5d. PROJECT NUMBER
M02R

5e. TASK NUMBER
20

5f. WORK UNIT NUMBER
00

7. PERFORMING ORGANIZATION NAME(S) AND ADDRESS(ES)

Metals Branch (AFRL/MLLM)
Metals, Ceramics, and Nondestructive Evaluation Division
Materials and Manufacturing Directorate
Air Force Research Laboratory, Air Force Materiel Command
Wright-Patterson Air Force Base, OH 45433-7750

Wright State University

Institute for Metals Superplasticity Problems

8. PERFORMING ORGANIZATION REPORT NUMBER
AFRL-ML-WP-TP-2004-400

9. SPONSORING/MONITORING AGENCY NAME(S) AND ADDRESS(ES)
Materials and Manufacturing Directorate
Air Force Research Laboratory
Air Force Materiel Command
Wright-Patterson Air Force Base, OH 45433-7750

10. SPONSORING/MONITORING AGENCY ACRONYM(S)
AFRL/MLLM

11. SPONSORING/MONITORING AGENCY REPORT NUMBER(S)
AFRL-ML-WP-TP-2004-400

12. DISTRIBUTION/AVAILABILITY STATEMENT
Approved for public release; distribution is unlimited.

13. SUPPLEMENTARY NOTES

ABSTRACT ***(Maximum 200 Words), ,***
The static-coarsening behavior of the alpha-beta titanium alloy, Ti-6Al-4V, was established via a series of heat treatments at typical forging-preheat and final-heat-treatment temperatures followed by quantitative metallography. For this purpose, samples of an ultra-fine-grain-size (UFG) billet with a microstructure of equiaxed alpha in a beta matrix were heated at temperatures of 843,900,955, and 982ºC for times between 0.25 and 144 h followed by water quenching. The coarsening of the primary alpha particles was found to follow r3-vs-time kinetics, typical of volume-diffusion-controlled behavior, at the three lower temperatures. At the highest temperature, the kinetics appeared to be fit equally well be an r3 of r4 dependence on time. The observations were interpreted in terms of the modified LSW theory considering the effects of volume fraction on kinetics and the fact that the phases are not terminal solid solutions. Prior models which take into account the overall source/sink effects of all particles on each other provided the best description of the observed dependence of coarsening on the volume fraction of primary alpha. In addition, the volume-diffusion kinetics derived for the UFG material were found to be capable of describing the coarsening behavior observed for industrial-scale billet of Ti-6Al-4V with a coarser starting equiaxed-alpha microstructure.

15. SUBJECT TERMS

16. SECURITY CLASSIFICATION OF:			17. LIMITATION OF ABSTRACT:	18. NUMBER OF PAGES	19a. NAME OF RESPONSIBLE PERSON (Monitor)
a. REPORT	b. ABSTRACT	c. THIS PAGE			Sheldon L. Semiatin
Unclassified	Unclassified	Unclassified	SAR	40	19b. TELEPHONE NUMBER *(Include Area Code)* (937) 255-1345

Standard Form 298 (Rev. 8-98)
Prescribed by ANSI Std. Z39-18

COARSENING BEHAVIOR OF AN ALPHA-BETA TITANIUM ALLOY

S.L. Semiatin, B.C. Kirby*, and G.A. Salishchev‡

Air Force Research Laboratory, Materials and Manufacturing Directorate,
AFRL/MLLM, Wright-Patterson Air Force Base, OH 45433-7817 USA
*Wright State University, Department of Mechanical Engineering,
Dayton, OH 45435 USA
‡Institute for Metals Superplasticity Problems, Ufa 450001,
Bashkortostan, Russia

ABSTRACT

The static-coarsening behavior of the alpha-beta titanium alloy, Ti-6Al-4V, was established via a series of heat treatments at typical forging-preheat and final-heat-treatment temperatures followed by quantitative metallography. For this purpose, samples of an ultra-fine-grain-size (UFG) billet with a microstructure of equiaxed alpha in a beta matrix were heated at temperatures of 843, 900, 955, and 982°C for times between 0.25 and 144 h followed by water quenching. The coarsening of the primary alpha particles was found to follow r^3 - vs - time kinetics, typical of volume-diffusion-controlled behavior, at the three lower temperatures. At the highest temperature, the kinetics appeared to be fit equally well by an r^3 or r^4 dependence on time. The observations were interpreted in terms of the modified LSW theory considering the effects of volume fraction on kinetics and the fact that the phases are not terminal solid solutions. Prior models which take into account the overall source/sink effects of all particles on each other provided the best description of the observed dependence of coarsening on the volume fraction of primary alpha. In addition, the volume-diffusion kinetics derived for the UFG material were found to be capable of describing the

coarsening behavior observed for industrial-scale billet of Ti-6Al-4V with a coarser starting equiaxed-alpha microstructure.

I. INTRODUCTION

The instability of microstructure in metallic materials during high-temperature exposure is of considerable interest from both a scientific and engineering perspective. For example, static grain growth, particle coarsening, spheroidization of a lamellar microstructure, and other processes may lead to substantial losses in both first and second tier mechanical properties, such as yield strength and creep resistance, during service exposure. Hence, a considerable amount of attention has focused on the phenomenological and mechanistic descriptions of such changes in microstructure [1, 2].

In two-phase alloys, the coarsening of a precipitate phase during high-temperature exposure has been examined in great detail, both experimentally and theoretically. Driven by the reduction in energy associated with the matrix-precipitate interfaces, coarsening comprises the growth of large particles and the shrinkage of smaller particles. Such so-called Ostwald-ripening processes were initially described in models developed by Greenwwood [3], Lifshitz and Slyosov [4], and Wagner [5], thus leading to a quantitative framework usually referred to as LSW theory. These approaches relied on a diffusion analysis in which the growth behavior of each particle is independent of the positions of all of the other particles and thus assumed a mean-field approximation in which the source/sink of solute is infinitely far away. The principal predictions of these models were (1) the cube of the average particle radius varies linearly with time, and (2) the

particle-radius distribution, when scaled by the average particle size, remains invariant with time (i.e., remains self-similar).

Strictly speaking, the LSW approach is valid only for systems comprising a dilute terminal solid solution and a vanishingly small volume fraction of second phase of essentially pure solute. Because of these restrictions, the LSW theory was subsequently expanded in a plethora of analyses. For example, Asimow [6], Sarian and Weart [7], Ardell [8], Brailsford and Wynblatt [9], and Voorhees and Glicksman [10, 11] described various analytic and computation approaches for coarsening problems involving finite volume fractions of second-phase particles. In particular, Voorhees and Glicksman used an elegant method based on potential theory to derive the solution to the diffusion problem comprising an array of particles each of which acts as a source or sink of solute.

When compared to experimental measurements, however, model predictions of the effect of volume fraction on coarsening tended to *overestimate* the observed rates for solid-solid systems (e.g., gamma-prime-strengthened nickel-base superalloys) except in limited instances and to *underestimate* the observed rates for systems comprising solid particles in a liquid matrix [12-15]. Such differences were attributed to the effect of factors such as elastic strain energy (due to misfit between the matrix and precipitate phases) [12, 16], initial particle-size distribution [17], and particle-coalescence (in liquid-solid systems) [18] on coarsening behavior. With regard to phase-composition effects, Calderon, et al. [19] provided an analysis which demonstrated that the coarsening rate in systems containing precipitates which are not terminal solid solutions can be

greater by an order of magnitude (or more) than that predicted by classical LSW theory.

The objective of the present work was to quantify and interpret the static-coarsening behavior in alpha-beta titanium alloys, a system that has not been investigated to a great extent despite the engineering importance of such materials. Static coarsening in titanium alloys is important because of its influence on the evolution of microstructure during thermomechanical processing (TMP), let alone its effect on final service properties. For instance, recent work has shown that the primary-alpha particle size developed during the numerous heating or forging operations which wrought titanium components undergo during TMP can have a very important influence on final heat treatment response in the alpha-beta phase field [20]. Furthermore, the coarsening of alpha particles can lead to measurable losses in both strength and ductility.

Titanium alloys are also excellent candidates for establishing the validity of various coarsening models because they contain a large volume fraction of primary phase (hcp alpha-phase particles) in a matrix of bcc beta phase; the volume fractions of the phases are easily adjusted by changing the heat treatment temperature. Furthermore, neither the alpha nor the beta phase is a terminal solid solution. To establish the coarsening behavior of alpha-beta titanium alloys, therefore, heat treatments were conducted on a specially prepared billet of ultra-fine grain (UFG) Ti-6Al-4V. The results were compared to coarsening measurements on a commercially produced billet of Ti-6Al-4V.

II. MATERIALS AND PROCEDURES

A. *Materials*

The present program utilized two lots of Ti-6Al-4V. The first lot comprised a billet measuring 150 mm diameter X 200 mm length fabricated at the Institute for Metals Superplasticity Problems (IMSP) (Ufa, Russia) [21, 22]. It had a measured composition (in weight percent) of 6.3 aluminum, 4.1 vanadium, 0.18 iron, 0.18 oxygen, 0.010 carbon, 0.010 nitrogen, 0.002 hydrogen, balance titanium, and a beta-transus temperature T_β (at which alpha + beta $\rightarrow$ beta) of 995°C. The billet had been produced by beta annealing a preform at 1010°C for one hour followed by water quenching to produce a fine, Widmanstatten-alpha microstructure. The preform was then warm worked at 600°C via forging along three orthogonal directions to a cumulative von Mises effective strain of approximately 3. By this means, an ultra-fine grain (UFG) microstructure of equiaxed alpha in a beta matrix was produced. The alpha particle size was approximately 2.5 μm. Transmission electron microscopy (TEM) revealed that alpha-alpha sub-boundaries were also developed within the alpha particles, thus indicating an alpha grain/subgrain size of ~0.5 μm (Figure 1a). However, after relatively short annealing times (of the order of 15-30 minutes) at elevated temperatures, almost all of the sub-boundaries appeared to have been eliminated, as indicated by the absence of channeling contrast in backscattered electron images (BSEI) shot in a scanning electron microscope (SEM) (Figures 1b-d). (Alpha-phase is the darker phase, and beta/transformed beta is the lighter phase in BSEI photographs of alpha-beta titanium alloys such as Ti-6Al-4V.) In

addition, some of the alpha particles appeared to consist of remnants of alpha lamellae not fully globularized by the warm working operation. These 'dog-leg' shaped particles (e.g., that marked by an arrow in Figure 1c) had internal alpha-alpha boundaries of very low misorientation as evidenced by their stability during long-term thermal exposure.

Although it had a coarser starting microstructure than the UFG material and thus enabled the evaluation of coarsening behavior over a narrower range of particle sizes, the second material was chosen to be representative of industrially produced Ti-6Al-4V. It was supplied by Timet Corporation (Henderson, NV) as 12.5-mm diameter x 150-mm length round bars of Ti-6Al-4V. The material had a measured composition (in weight percent) of 6.4 aluminum, 4.2 vanadium, 0.14 iron, 0.19 oxygen, 0.016 carbon, 0.0040 hydrogen, 0.005 nitrogen, the balance being titanium. Each bar had been cut from the mid-radius of 200-mm-diameter forging-bar stock produced using typical mill practices for the alloy. The beta-transus temperature was determined via a series of heat treatments to be 1000°C. The room-temperature microstructure of this material comprised equiaxed alpha grains ~12 μm in diameter in a beta matrix (Figure 2).

B. *Procedures*

Cylindrical samples measuring 12.5 diameter X 12.5 mm length were cut from both lots of Ti-6Al-4V and heat treated to establish the kinetics of coarsening at various temperatures. Samples of the UFG Ti-6Al-4V were enclosed in evacuated quartz capsules back filled with argon and heat treated at 843°C (for 1, 4, 24, or 72 hours), 900°C (for 1, 4, 16, 48, or 144 hours), 955°C

(for 0.25, 1, 4 16, or 48 hours), or 982°C (for 0.25, 4, 24, or 48 hours). Each capsule was water quenched following heat treatment. Only a limited number of heat treatments were conducted on the commercially produced Ti-6Al-4V in order to compare its coarsening kinetics with those for the UFG material. To this end, samples of the commercially produced material were similarly encapsulated and heat treated at 955°C for 4, 16, or 64 hours followed by water quenching.

Following heat treatment, each sample was sectioned and prepared using standard metallographic techniques. A series of BSEI photographs was then shot at several magnifications. For each heat-treatment condition, 4 to 6 micrographs were analyzed, thus insuring that ~600-1000 particles were sampled. The average alpha particle size, A_α was determined by counting the number of particles, N_α, and measuring the volume fraction of alpha, f_α, in each micrograph and applying the relation $A_\alpha = f_\alpha A_T / N_\alpha$, in which A_T denotes the area of the micrograph. Those particles consisting of a 'dog-leg' geometry were counted as being 1.5 particles in number to provide an approximate estimate of the effect of their radii of curvature on coarsening behavior. The average particle radius, $\bar{r}_\alpha$, was estimated from the value of A_α based on a circle with equivalent area. Because only first-order coarsening behavior was of interest, a factor to correct for stereological effects [23] was not utilized.

In addition to the determination of average particle size, a number of micrographs for the UFG Ti-6Al-4V heat treated at 900 or 955°C were analyzed to determine the particle-size distribution. This was accomplished by determining the number of pixels for each alpha particle in hand-painted digital images. Size-

distribution histograms thus determined were normalized (to yield unit area under the corresponding fitted curve) to permit comparison with previous measurements and model predictions.

III. RESULTS AND DISCUSSION

The principal results of this work comprised the measurement of coarsening kinetics for the two lots of Ti-6Al-4V and the interpretation of these measurements in terms of prior models treating the effect of volume fraction and phase composition on coarsening behavior.

A. *Coarsening Observations and Kinetics*

Microstructure observations revealed marked changes in the alpha particle size during heat treatment. This was evidenced by micrographs shot at the same magnification for heat treatments of various durations at each temperature (e.g., Figures 3 and 4). The self-similarity of microstructure with heat treatment time, a behavior which is predicted by classical coarsening theories, was also evident in micrographs taken at different magnifications (e.g., Figure 5).

The functional form of the variation of average alpha particle radius $\bar{r}_\alpha$ with time t was deduced by plotting the measurements in terms of $\bar{r}_\alpha^n - \bar{r}_{\alpha o}^n$ versus $t - t_o$ (in which $\bar{r}_{\alpha o}$ $(t = t_o)$ denotes the average particle radius at the initial time t_o) for various values of the coarsening exponent n. An example for a heat treatment temperature of 900°C is shown in Figure 6. The curvature of these plots changed from concave down to concave up with increasing n. The relation

between $\bar{r}_\alpha^n - \bar{r}_{\alpha o}^n$ and $t - t_o$ was closest to linear for n = 3. Similar series of plots also revealed that a fit based on n = 3 was closest to producing a linear relationship for heat treatment temperatures of 843 and 955°C. At 982°C, on the other hand, both n = 3 and n = 4 gave fits that were slightly concave down. However, an approximate linear fit could still be obtained with n = 3 at this temperature.

In Figure 7, the n = 3 fits (and the corresponding data points) are summarized for the UFG Ti-6Al-4V material. Not surprisingly, the slope, k, of these plots increased as the temperature increased from 843°C to 900°C to 955°C. However, the results for 982°C lay close to those for 900°C, i.e., between 843 and 955°C.

The coarsening response for the commercially produced Ti-6Al-4V heat treated at 955°C was compared to the corresponding results for the UFG material. For this purpose, the value of $t - t_o$ for the UFG material at which the value of $\bar{r}_\alpha$ was equal to $\bar{r}_\alpha(4h)$ for the commercially produced alloy was determined. The measured values of $\bar{r}_\alpha(16\ h)$ and $\bar{r}_\alpha(64h)$ for the commercially produced material were then plotted at time increments of 12 and 60 hours, respectively, relative to this specific value of $t - t_o$, assuming the same value of $\bar{r}_{\alpha o}$ as the UFG material. This comparison (Figure 8) showed excellent agreement for the two lots of material.

Particle-size measurements for UFG Ti-6Al-4V samples heat treated at 900°C (Figure 9) and 955°C (Figure 10) revealed that the overall distributions

was essentially self similar, i.e., invariant with time when plotted in terms of the normalized alpha particle size (i.e., $r_\alpha / \bar{r}_\alpha$). The plots revealed that the maximum value of $r_\alpha / \bar{r}_\alpha$ was slightly below 2 at both temperatures and that the peak in the distribution was approximately 1.25 at 900°C and 1.05 at 955°C.

B. *Interpretation of Coarsening Kinetics*

1. Coarsening Mechanism

The observed kinetics of coarsening for Ti-6Al-4V were interpreted in terms of the classical LSW theory as modified for finite volume fraction effects and matrix/particle compositions which are not terminal solid solutions. For coarsening controlled by bulk diffusion of a solute through a matrix denoted as β, the classical LSW theory predicts the following for the variation of the average particle radius as a function of time:

$$\bar{r}_\alpha^3 - \bar{r}_{\alpha o}^3 = \left[\frac{8D\gamma_{\alpha\beta}C_\beta V_M}{9RT}\right](t - t_o) = k_{LSW}(t - t_o)\,, \qquad (1)$$

in which D denotes the diffusivity in the beta matrix of the rate limiting solute, $\gamma_{\alpha\beta}$ is the energy associated with particle-matrix (alpha-beta) interfaces (in J/m^2), C_β is the *equilibrium* concentration in the beta matrix of the rate-limiting solute (expressed as an atomic fraction), V_M is the molar volume of the precipitate, R is the universal gas constant, and T is the absolute temperature. The LSW rate constant k_{Lsw} is thus defined as follows:

$$k_{LSW} \equiv \frac{8D\gamma_{\alpha\beta}C_\beta V_M}{9RT}\,. \qquad (2)$$

The form of the rate constant, k_{MLSW}, for a finite volume fraction of particles in a system comprising two concentrated alloy phases is the following [19, 24]:

$$k_{MLSW} = \frac{8f(\phi)D\gamma_{\alpha\beta}C_\beta(1-C_\beta)V_M}{9RT(C_\alpha-C_\beta)^2[1+\partial \ln r/\partial \ln C_\beta]}, \qquad (3)$$

in which $f(\phi)$ describes the functional dependence of the rate constant on volume fraction ϕ, C_α is the *equilibrium* concentration in the alpha particle of the rate-limiting solute (expressed as an atomic fraction), and r is the activity coefficient of the rate-limiting solute in the beta matrix. As summarized by Doherty [24], the terms in Equation (3) which are related to the volume-fraction function f and the phase concentrations can readily increase the magnitude of predictions of the rate constant by one or two orders of magnitude.

In the present work, the measured coarsening kinetics exhibited an $\bar{r}_\alpha^3 - \bar{r}_{\alpha o}^3$ versus $t - t_o$ behavior, thus suggestive of coarsening controlled by bulk-diffusion through the beta matrix.* In addition, the particle-size distributions after different annealing times were approximately self-similar when normalized by the average particle radius and were similar to those predicted by LSW-type models.

---

*High magnification photographs (not shown) revealed that the faceted nature of some of the alpha-particle boundaries was associated with triple points formed by the alpha and beta phases. The very rapid growth of beta grains [25] relative to the measured times for coarsening of primary alpha indicates that beta grain growth is *not* the rate-limiting step in the evolution of microstructure. Furthermore, a comparison of boundary and bulk diffusivities for beta titanium [26] suggests that that mass transport through the beta lattice predominates in the overall diffusion process at the heat treatment temperatures used in the present work.

Hence, the measured rate constants, k, were compared to the theoretical predictions described by Equation (3).

2. Input Data for Estimating Coarsening Rate Constant

As shown by Equation (3), the input data required to predict the coarsening rate constant include the values of the equilibrium phase concentrations, the solute diffusivity, molar volume, alpha-beta interface energy, and the thermodynamic factor (= $1 + \partial \ln r / \partial \ln C_\beta$). The values for the equilibrium compositions of the alpha and beta phases (Table I) were taken from Reference 20. These values had been determined from wavelength-dispersive spectroscopy on Ti-6Al-4V samples cut from the same commercially produced billet of Ti-6Al-4V used in the present work. The samples had been heat treated for long times to produce coarse alpha-particle sizes. Even though thermodynamic equilibrium would have mandated an infinite particle size (i.e., flat alpha-beta interfaces), it is believed that the values obtained provide a reasonable estimate of the phase compositions. The thermodynamic factors for aluminum and vanadium solutes in beta titanium at the pertinent heat-treatment temperatures were also taken from previous work [20]. For the phase compositions of interest, this factor is equal to approximately 2 (aluminum) or 1 (vanadium).

The diffusion coefficients for aluminum and vanadium solutes in the beta phase of Ti-6Al-4V were obtained from Reference 27. These diffusivities were determined from diffusion-couple experiments using ternary alloys (plus interstitial elements) with compositions comparable to the beta phase in Ti-6Al-

4V. For each couple, the content of either Al or V was varied while holding that of the other substitutional element fixed. The measured diffusivities were as follows:

$$\text{Aluminum: } D^{\beta}_{Al}(\mu m^2/s) = 199200 \exp(-18040/T(K)) \quad (4a)$$

$$\text{Vanadium: } D^{\beta}_{V}(\mu m^2/s) = 77000 \exp(-17460/T(K)) \quad (4b)$$

The molar volume of alpha particles, 10,440 mm^3, was determined from the mass of one mole of Ti-0.123Al-0.0185V (in atomic-fraction terms) (i.e., 45.39 g) and the density of the alpha phase at the heat treatment temperatures used in the present work (i.e., 4347 kg/m^3).

The final property required for estimating the coarsening rate constant (exclusive of the volume fraction function $f(\phi)$) was the alpha-beta interface energy $\gamma_{\alpha\beta}$. Unfortunately, the value of this energy appears not to have been reported in the literature. Nevertheless, its value was estimated from the fact that the alpha-beta interface is most likely an incoherent one produced during the large-strain deformation required to globularize the colony-alpha microstructure in alpha-beta titanium alloys produced via an ingot-metallurgy route. In such cases, reasonable values for $\gamma_{\alpha\beta}$ lie in the range of 0.2 – 0.4 J/m^2 [1]. Therefore calculations were done for $\gamma_{\alpha\beta}$ = 0.2 J/m^2 and $\gamma_{\alpha\beta}$ = 0.4 J/m^2.

3. Comparison of Measured and Predicted Rate Constants

Measured coarsening-rate constants were compared to predictions based on Equation (3) and previous models for the volume fraction function $f(\phi)$. Initial attention focused on estimates of the coarsening rate, k_{MLSW}, *assuming that the volume fraction correction ($f(\phi)$) is unity for all volume fractions ϕ.* The results of

these calculations are summarized in Tables II and III, assuming that diffusion of aluminum or vanadium is the rate-limiting process, respectively. The calculations revealed that the composition term in the expression for k_{MLSW} (i.e., $C_\beta(1-C_\beta)/(C_\alpha - C_\beta)^2$) is approximately three orders of magnitude greater than the corresponding term, C_β, for k_{LSW}, thus underscoring the importance of taking composition effects into account in the analysis of coarsening. A comparison of the results in Tables II and III also indicated that the predicted coarsening rates for a given value of $\gamma_{\alpha\beta}$ are 2 to 3 times *greater* for aluminum diffusion than for vanadium diffusion. Hence, it is concluded that vanadium diffusion controls the overall coarsening rate.

The values of the ratio of measured-to-predicted coarsening rates for the case of vanadium-diffusion control show a noticeable dependence on volume fraction (Table III). For $\gamma_{\alpha\beta}$ = 0.2 J/m^2, this ratio varies from approximately unity at low volume fractions of alpha (f_α ~0.05) to a value of ~13 at a volume fraction equal to 0.71. For $\gamma_{\alpha\beta}$ = 0.4 J/m^2, the ratio of measured-to-predicted coarsening rates for the same range of volume fractions varies from ~0.5 to ~7. These ratios provide estimates of the function $f(\phi)$ and were therefore compared to predictions from previous models as summarized by Voorhees and Glicksman [11]. The various trends of prior analytical and numerical models for $f(\phi)$ are shown in Figure 11, taken from Reference 11. The present values of the ratio of measured-to-predicted k's for $\gamma_{\alpha\beta}$ = 0.4 J/m^2, which appear to be closest to the predicted trend lines, are also plotted in this figure. A comparison of the models and the data for Ti-6Al-4V shows that the predictions of Voorhees and Glicksman

[11] and, to a lesser extent, those of Brailsford and Wynblatt [9] provide a reasonable first order correlation with the present observations. The most pertinent deviation from these models appears to be the datum for 982°C for which $\phi \sim 0.05$. At this volume fraction, the measured rate constant should be close to the value of k_{MLSW} with f = 1, yielding a ratio of unity in Figure 11. The fact that the actual ratio was ~0.5 may be a result of the finding that the coarsening measurements for this temperature followed a slightly concave down behavior when fit by n =3 or n=4. The linear fit used here would therefore tend to underestimate the experimental rate constant at short times and overestimate it at long times. Hence, if attention were focused solely on the short-time behavior, the ratio would then be close to unity at 982°C.

The agreement shown in Figure 11 is particularly encouraging (at least for the present alloy system) in light of the general tendency for the various volume-fraction-effect models to either greatly underestimate or overestimate observed behaviors. The fact that the models of Voorhees and Glicksman [11] and Brailsford and Wynblatt [9] yield the best agreement is not surprising in view of the fact that their approaches account for the short and long range influence on the diffusion field of the source/sink behavior of a collection of particles. By specifying the solute concentration at the boundaries of representative, single-particle cells, other models, such as those described by Asimow [6] and Ardell [8], assume that the interaction of the diffusion fields around particles is extremely localized, thereby leading to an exaggerated effect of volume fraction on coarsening rate.

4. Comparison of Measured and Predicted Particle-Size Distributions

The comparison of measured and predicted size distributions is not as straightforward as the rate constant because of the non-spherical nature of the alpha particles. Such shapes complicate the correlation between the intercept length for each particle (the quantity which is measured on a two-dimensional section) and the actual particle radius. Nonetheless, some qualitative conclusions can be drawn regarding the measurements at 900°C and 955°C.

The particles at 900°C (Figure 3, 5a,b) appear somewhat cuboidal/ polyhedral. Hence, a section away from the centroid of such shapes probably produces a characteristic particle dimension which is close to the effective 'radius'. In this case, the measured particle-size distribution (Figure 9) can be compared directly to model predictions of the particle-radius distribution. For a volume fraction of 0.50, which is close to that in Ti-6Al-4V at 900°C, Voorhees and Glicksman [11] predicted a peak in the particle-radius distribution of ~1.2 and a maximum value of $r_\alpha / \bar{r}_\alpha$ equal to ~2. To a good first approximation, the measurements (Figure 9) mirror such predictions.

For a volume fraction of ~0.25, Voorhees and Glicksman [11] predicted a peak of ~1.65 in the distribution of particle radii and a 'tail' in the distribution at $r_\alpha / \bar{r}_\alpha$ ~ 1.5. This peak is much *greater* than the measured value of ~1, and the tail is at a much *lower* value than the measurement of ~2 for Ti-6Al-4V heat treated at 955°C at which ϕ = 0.25 (Figure 10). The particles at 955°C (Figures 4, 5c,d) appear somewhat more spheroidal than those at 900°C, however. Hence,

the 955°C measurements should be compared to the corresponding intercept distribution. In terms of intercept distribution, Hardy and Voorhees [15] have shown that the Voorhees-and-Glicksman peak is ~0.85 and the tail is ~2.3 for ϕ = 0.50. This value of the distribution peak is slightly *lower* than that observed, and the tail is at a value of $r_\alpha / \bar{r}_\alpha$ slightly *greater* than that measured. The comparison of the measured and predicted size distributions at 955°C thus suggests that more detailed stereological characterization of the observed alpha-particle sizes and a Voorhees-and-Glicksman-type model that treats irregular particle shapes may provide improved agreement. In addition, the possibly larger values of the true particle radius at 955°C (and perhaps 982°C) inferred from this analysis would give ride to somewhat larger values of the measured coarsening rate and thus values of $f(\phi)$ closer to the Voorhees-and-Glicksman predictions at these temperatures.

IV. SUMMARY AND CONCLUSIONS

A series of heat treatments was conducted on two lots of Ti-6Al-4V with different initial primary-alpha particle sizes to quantify static coarsening behavior for a typical alpha-beta titanium alloy. The following conclusions were drawn:

1. Static coarsening of the primary alpha phase in Ti-6Al-4V follows classical bulk-diffusion controlled kinetics characterized by $\bar{r}_\alpha^3 - \bar{r}_{\alpha o}^3$ versus time behavior and particle-size distributions which maintain self-similarity during the coarsening reaction.

2. The coarsening rate constant can be predicted from modified LSW theory by taking proper account of the equilibrium compositions of the alpha and beta (matrix) phases, material coefficients (diffusivity, alpha-beta interface energy, molar volume), and volume-fraction effects.
3. For Ti-6Al-4V, the coarsening kinetics are controlled by the diffusion of vanadium solutes through the beta matrix.
4. Models, such as that developed by Voorhees and Glicksman [10, 11], which treat the source/sink effects of large aggregates of second-phase particles, provide the best quantitative description of the effect of volume fraction on coarsening behavior for the Ti-6Al-4V alloy.

Acknowledgements – This work was conducted as part of joint research of the Metals Processing Group of the Air Force Research Laboratory's Materials and Manufacturing Directorate and the Institute for Metals Superplasticity Problems. The support and encouragement of the laboratory management and the Air Force Office of Scientific Research (Drs. C. S. Hartley and C.H. Ward, program managers) are gratefully acknowledged. The project effort was also partly conducted in support of the Air Force Metals Affordability Initiative program on Microstructure and Mechanical Property Modeling for Wrought Titanium Alloys being led by Ladish Company, Cudahy, WI. Two of the authors were supported under the auspices of AF Contract F33615-02-2-5800 (BCK) and ISTC/EOARD Partner Project 2124p (GAS). Technical discussions with Dr. D.U. Furrer (Ladish Company), Drs. S.P. Fox and V. Venkatesh (Timet Corporation), and Professor R.D. Doherty (Drexel University) are gratefully acknowledged.

References

1. J.W. Martin, R.D. Doherty, and B. Cantor: *Stability of Microstructure in Metallic Systems*, Cambridge University Press, Cambridge, UK, 1997.
2 M. McLean: *Metal Sci.*, 1978, vol. 12, pp. 113-122.
3. G.W. Greenwood: *Acta Metall.*, 1956, vol. 4, pp. 243-248.

4. I.M. Lifshitz and V.V. Slyozov: *J. Phys. Chem. Solids*, 1961, vol. 19, pp. 35-51.
5. C. Wagner: *Zeit. Elektrochem.*, 1961, vol. 65, pp. 581-591.
6. R. Asimow: *Acta Metall.*, 1963, vol. 11, pp.72-73.
7. S. Sarian and H.W. Weart: *J.Appl. Phys.*, 1966, vol. 37, pp. 1675-1681.
8. A.J. Ardell: *Acta Metall.*, 1972, vol. 20, pp. 61-71.
9. A.D. Brailsford and P. Wynblatt: *Acta Metall.*, 1979, vol. 27, pp. 489-497.
10. P.W. Voorhees and M.E. Glicksman: *Acta Metall.*, 1984, vol. 32, pp. 2001-2011.
11. P.W. Voorhees and M.E. Glicksman: *Acta Metall.*, 1984, vol. 32, pp. 2013-2030.
12. A.J. Ardell: *Scripta Metall. et Mater.*, 1990, vol. 24, pp. 343-346.
13. C.H. Kang and D.N. Yoon: *Metall. Trans. A*, 1981, vol. 12A, pp. 65-69.
14. S.S. Kang and D.N. Yoon: *Metall. Trans. A*, 1982, vol. 13A, pp. 1405-1411.
15. S.C. Hardy and P.W. Voorhees: *Metall. Trans. A*, 1988, vol. 19A, pp. 2713-2721.
16. A. Baldan: *J. Mat. Sci.*, 2002, vol. 37, pp. 2379-2405.
17. Z. Fang and B.R. Patterson: *Acta Metall. et Mater.*, 1993, vol. 41, pp. 2017-2024.
18. A.N. Niemi and T.H. Courtney: *J. Mat. Sci.*, 1981, vol. 16, pp. 226-236.
19. H. A. Calderon, P.W. Voorhees, J.L. Murray, and G. Kostorz: *Acta Metall. et Mater.*, 1994, vol. 42, pp. 991-1000.

20. S.L. Semiatin, S.L. Knisley, P.N. Fagin, F. Zhang, and D.R. Barker: *Metall. Mater. Trans. A*, 2003, vol. 34, pp. 2377-2386.

21. S.V. Zherebstov, G.A. Salishchev, R.M. Galeyev, O.R. Valiakhmetov, and S.L. Semiatin, "Formation of Submicrocrystalline Structure in Large-Scale Ti-6Al-4V Billet During Warm Severe Plastic Deformation," *Proc. Nano SPD2*, 2004, in press.

22. G.A. Salishchev, S.V. Zherebtsov, O.R. Valiakhmetov, R.M. Galeyev, V.K. Berdin, and S.L. Semiatin, *Ti-2003: Science and Technology*, G. Luetjering, ed., Wiley-VCH Verlag GmbH, 2004, in press.

23. E.E. Underwood: *Metals Handbook, Volume 9: Metallography and Microstructures*, Ninth Edition, ASM International, Materials Park, OH, 1985, pp. 123-134.

24. R.D. Doherty: in *Physical Metallurgy*, R.W. Cahn and P. Haasen, eds., North-Holland, Amsterdam, 1996, ch. 15.

25. S.L. Semiatin, J.C. Soper, and I.M. Sukonnik: *Acta Metall. Mater.*, 1996, vol. 44, pp. 1979-1986.

26. H.J. Frost and M.F. Ashby: *Deformation Mechanism Maps*, Pergamon Press, Oxford, UK, 1982, ch. 6.

27. S.L. Semiatin, T.M. Brown, T.A. Goff, P.N. Fagin, D.R. Barker, R.E. Turner, J.M. Murry, J.D. Miller, and F. Zhang: paper submitted to *Metall. Mater. Trans. A*, 2003.

Table I. Equilibrium Composition (Atomic Fraction) of the Alpha and Beta Phases in Ti-6Al-4V

Temperature (°C)	C_{Al}^{α}	C_{V}^{α}	C_{Al}^{β}	C_{V}^{β}
843	0.1232	0.0193	0.0802	0.0832
900	0.1232	0.0195	0.0908	0.0636
955	0.1232	0.0183	0.1033	0.0447
982	0.1232	0.0169	0.1057	0.0409

Table II. Comparison of Measured Coarsening Rates with Predictions* Based on Aluminum Diffusion

Temp (°C)	v/o α	Comp Term	Meas. k ($\mu m^3/h$)	K_{MLSW} ($\mu m^3/h$) $\gamma_{\alpha\beta}$ = 0.2 J/m^2	Ratio	K_{MLSW} ($\mu m^3/h$) $\gamma_{\alpha\beta}$ = 0.4 J/m^2	Ratio
843	0.71	39.9	2.18	0.274	7.96	0.549	3.98
900	0.56	78.6	5.95	1.108	5.37	2.216	2.69
955	0.26	233.9	7.59	6.316	1.20	12.63	0.61
982	0.05	308.7	3.45	11.283	0.31	22.57	0.15

* Predictions assuming $f(\phi) = 1$

Table III. Comparison of Measured Coarsening Rates with Predictions* Based on Vanadium Diffusion

Temp (°C)	v/o α	Comp Term	Meas. k ($\mu m^3/h$)	K_{MLSW} ($\mu m^3/h$) $\gamma_{\alpha\beta}$ = 0.2 J/m^2	Ratio	K_{MLSW} ($\mu m^3/h$) $\gamma_{\alpha\beta}$ = 0.4 J/m^2	Ratio
843	0.71	18.68	2.18	0.167	13.1	0.334	6.54
900	0.56	30.62	5.95	0.547	10.9	1.094	5.44
955	0.26	61.27	7.59	2.051	3.70	4.103	1.85
982	0.05	68.10	3.45	3.055	1.13	6.110	0.56

* Predictions assuming $f(\phi) = 1$

Figure Captions

Figure 1. Microstructure of UFG Ti-6Al-4V billet produced by IMSP: (a) TEM micrograph of as-received material and SEM micrographs of material water quenched after a 30-minute heat treatment at (b) 815°C, (c) 900°C, or (d) 955°C.

Figure 2. As-received microstructure of commercially-produced Ti-6Al-4V billet.

Figure 3. Backscattered electron images of the microstructure developed in UFG Ti-6Al-4V during heat treatment at 900°C for times of (a) 1, (b) 4, (c) 16, (d) 48, or (e) 144 hours. All of the micrographs were shot at the same magnification.

Figure 4. Backscattered electron images of the microstructure developed in UFG Ti-6Al-4V during heat treatment at 955°C for times of (a) 0.25, (b) 1, (c) 4, (d) 16, or (e) 48 hours. All of the micrographs were shot at the same magnification.

Figure 5. Backscattered electron images illustrating the self-similarity of the microstructure developed in UFG Ti-6Al-4V during heat treatments of (a) 900°C, 1h (b) 900°C, 144h, (c) 955°C, 0.25h, or (b) 955°C, 48h.

Figure 6. Plots of $\bar{r}_{\alpha}^{n} - \bar{r}_{\alpha o}^{n}$ versus $t - t_o$ for heat treatments of UFG Ti-6Al-4V at 900°C and values of n equal to (a) 1, (b) 2, (c) 3, and (d) 4.

Figure 7. Plots of $\bar{r}_{\alpha}^{3} - \bar{r}_{\alpha o}^{3}$ versus $t - t_o$ for heat treatments of UFG Ti-6Al-4V at various temperatures.

Figure 8. Comparison of the coarsening behavior of UFG Ti-6Al-4V and commercially-produced Ti-6Al-4V during heat treatment at 955°C.

Figure 9. Particle-size distributions for UFG Ti-6Al-4V heat treated at 900°C for (a) 1h, (b) 16 h, and (c) 144 h.

Figure 10. Particle-size distributions for UFG Ti-6Al-4V heat treated at 955°C for (a) 0.25 h, (b) 4 h, and (c) 48 h.

Figure 11. Comparison of model predictions of $f(\phi)$ [11] and the present results assuming $\gamma_{\alpha\beta} = 0.4$ J/m^2.

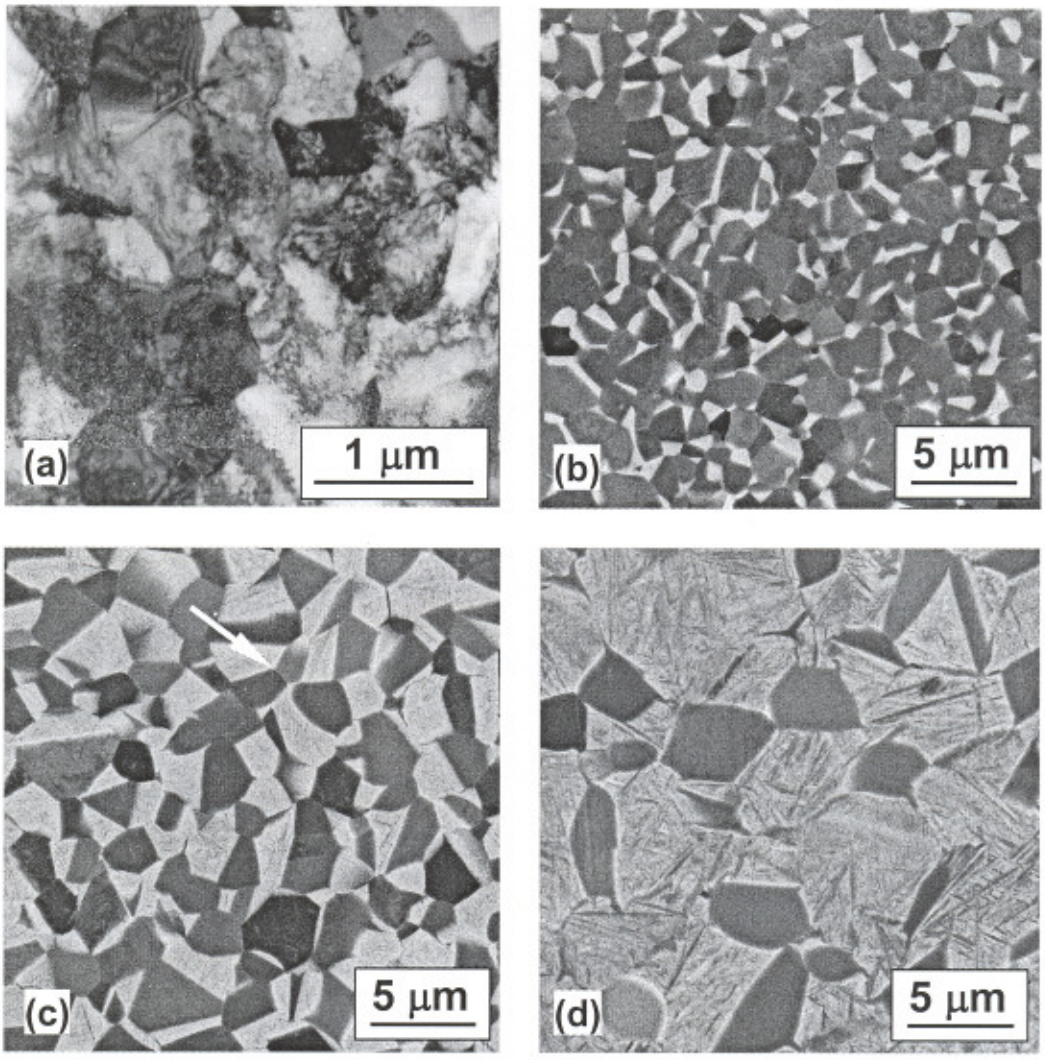

Figure 1. Microstructure of UFG Ti-6Al-4V billet produced by IMSP: (a) TEM micrograph of as-received material and SEM micrographs of material water quenched after a 30-minute heat treatment at (b) 815°C, (c) 900°C, or (d) 955°C.

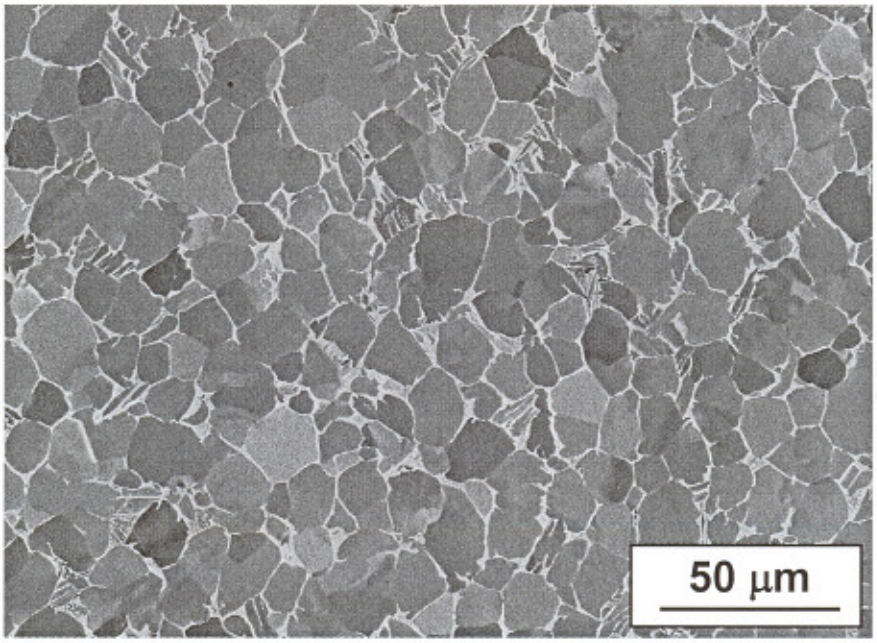

Figure 2. As-received microstructure of commercially-produced Ti-6Al-4V billet.

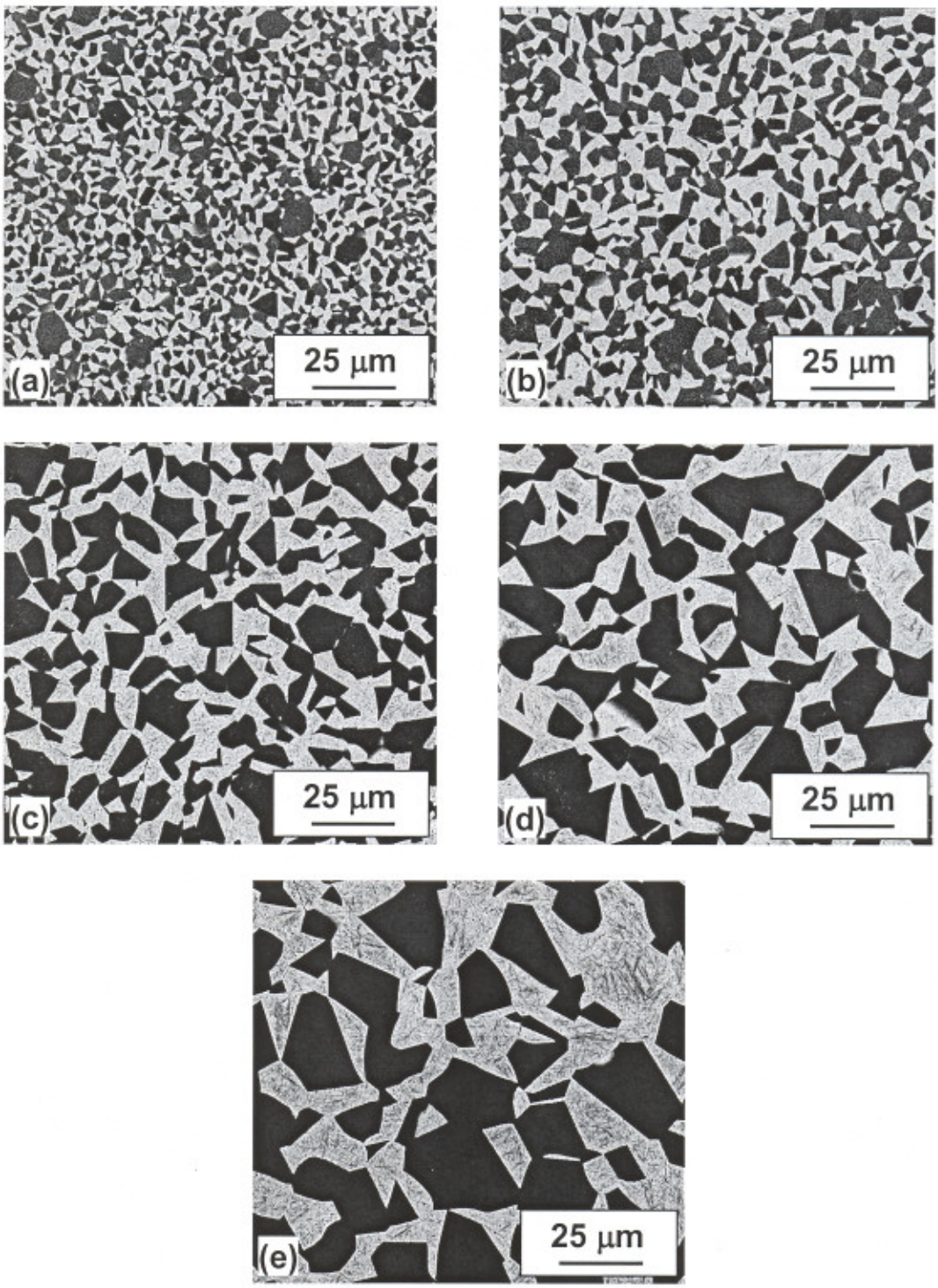

Figure 3. Backscattered electron images of the microstructure developed in UFG Ti-6Al-4V during heat treatment at 900°C for times of (a) 1, (b) 4, (c) 16, (d) 48, or (e) 144 hours. All of the micrographs were shot at the same magnification.

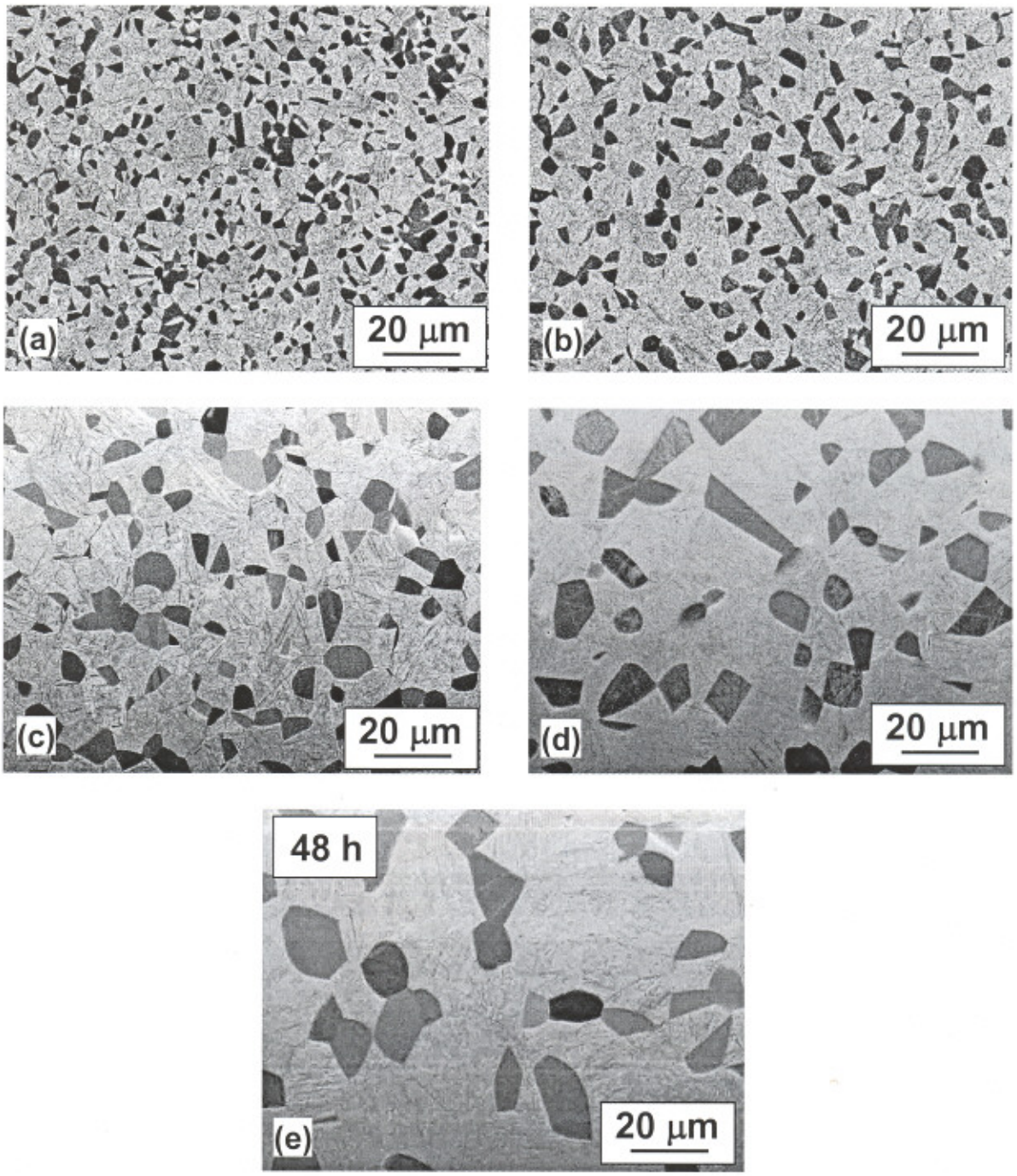

Figure 4. Backscattered electron images of the microstructure developed in UFG Ti-6Al-4V during heat treatment at 955°C for times of (a) 0.25, (b) 1, (c) 4, (d) 16, or (e) 48 hours. All of the micrographs were shot at the same magnification.

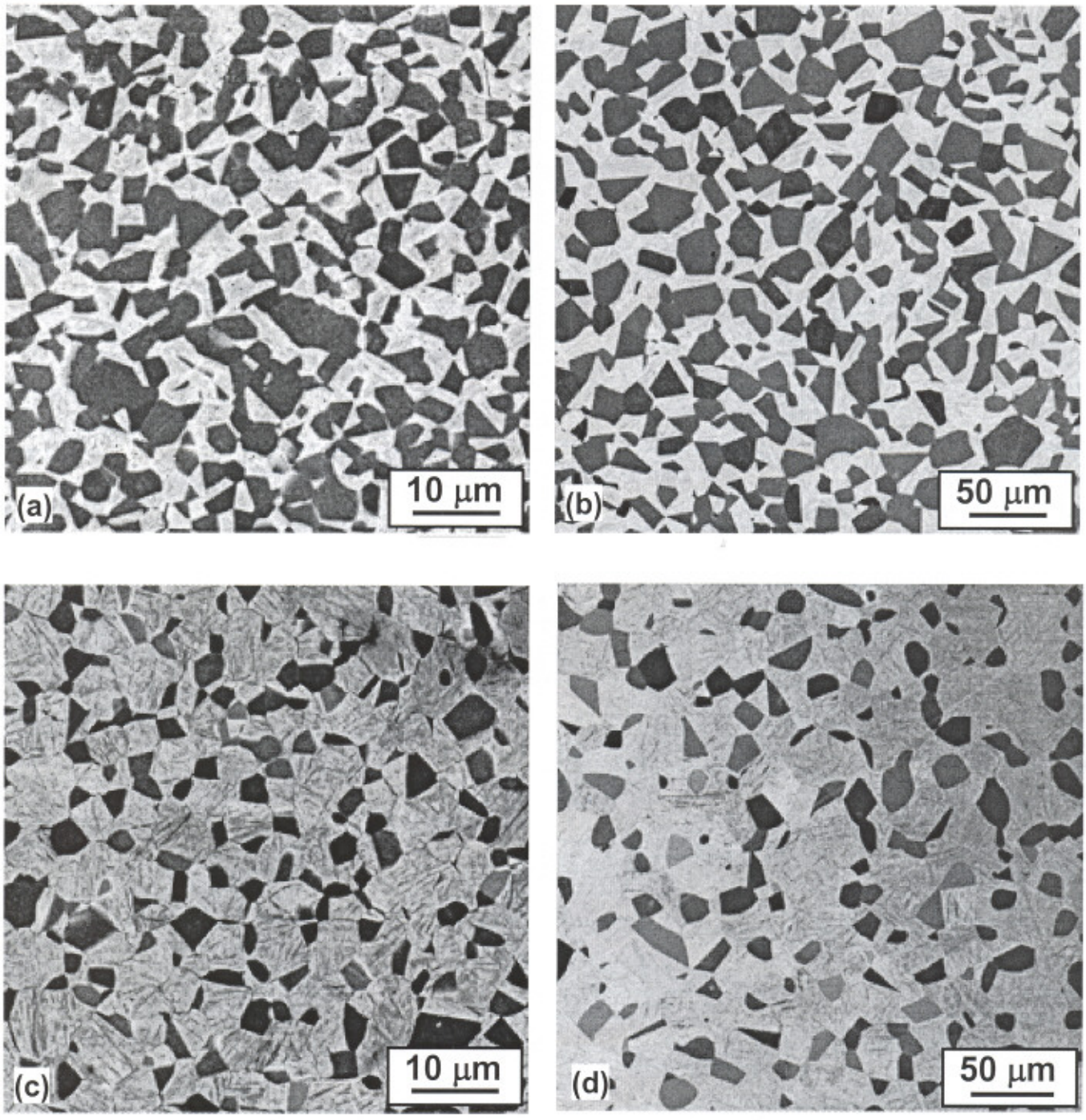

Figure 5. Backscattered electron images illustrating the self-similarity of the microstructure developed in UFG Ti-6Al-4V during heat treatments of (a) 900°C, 1h (b) 900°C, 144h, (c) 955°C, 0.25h, or (b) 955°C, 48h.

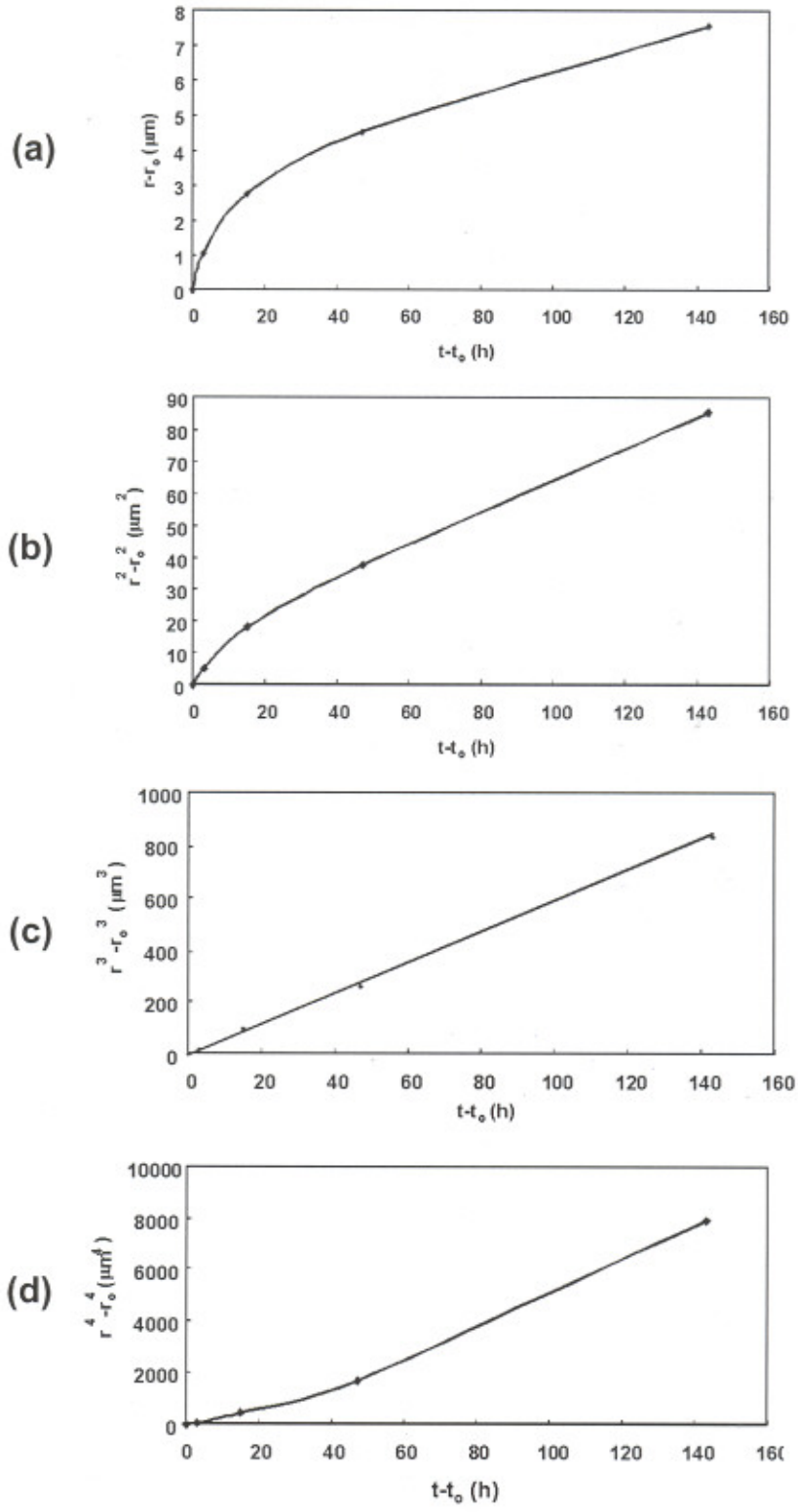

Figure 6. Plots of $\bar{r}_\alpha^n - \bar{r}_{\alpha o}^n$ versus $t - t_o$ for heat treatments of UFG Ti-6Al-4V at 900°C and values of n equal to (a) 1, (b) 2, (c) 3, and (d) 4.

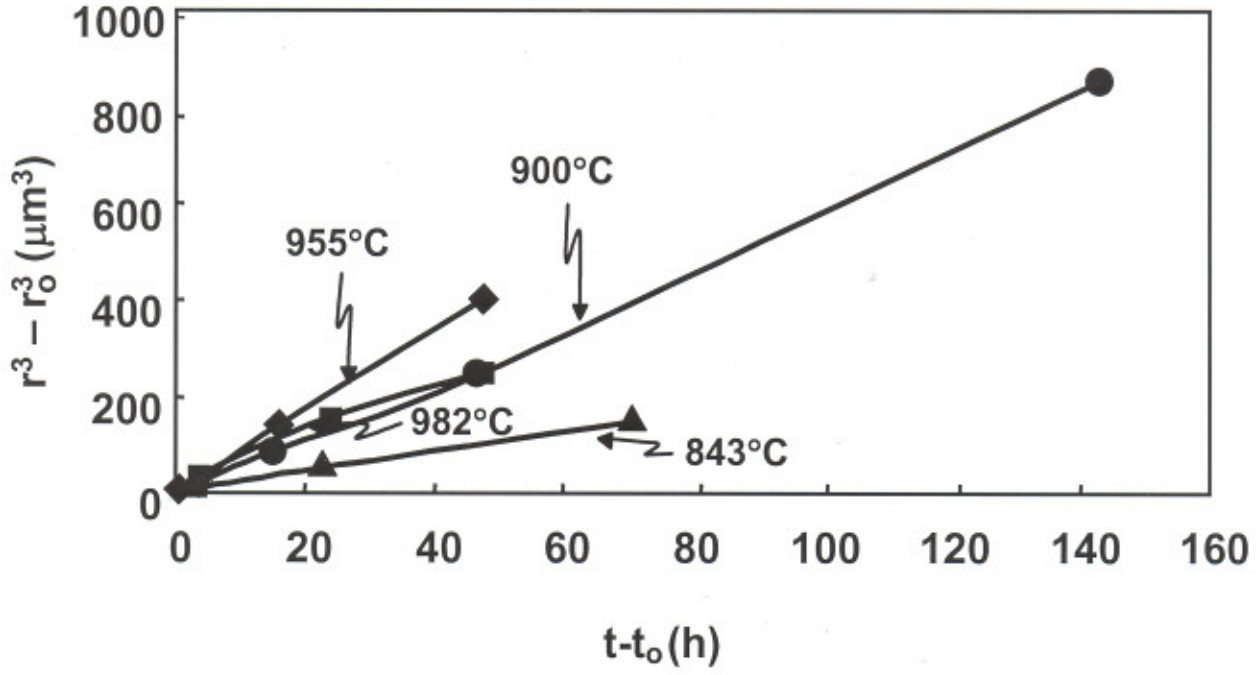

Figure 7. Plots of $\bar{r}_\alpha^3 - \bar{r}_{\alpha o}^3$ versus $t - t_o$ for heat treatments of UFG Ti-6Al-4V at various temperatures.

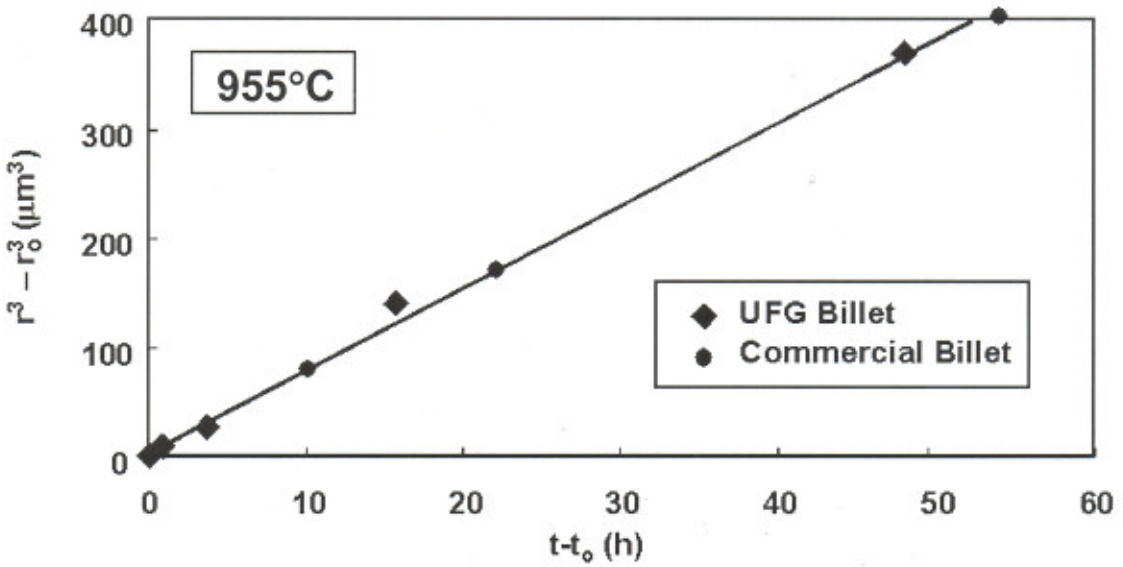

Figure 8. Comparison of the coarsening behavior of UFG Ti-6Al-4V and commercially-produced Ti-6Al-4V during heat treatment at 955°C.

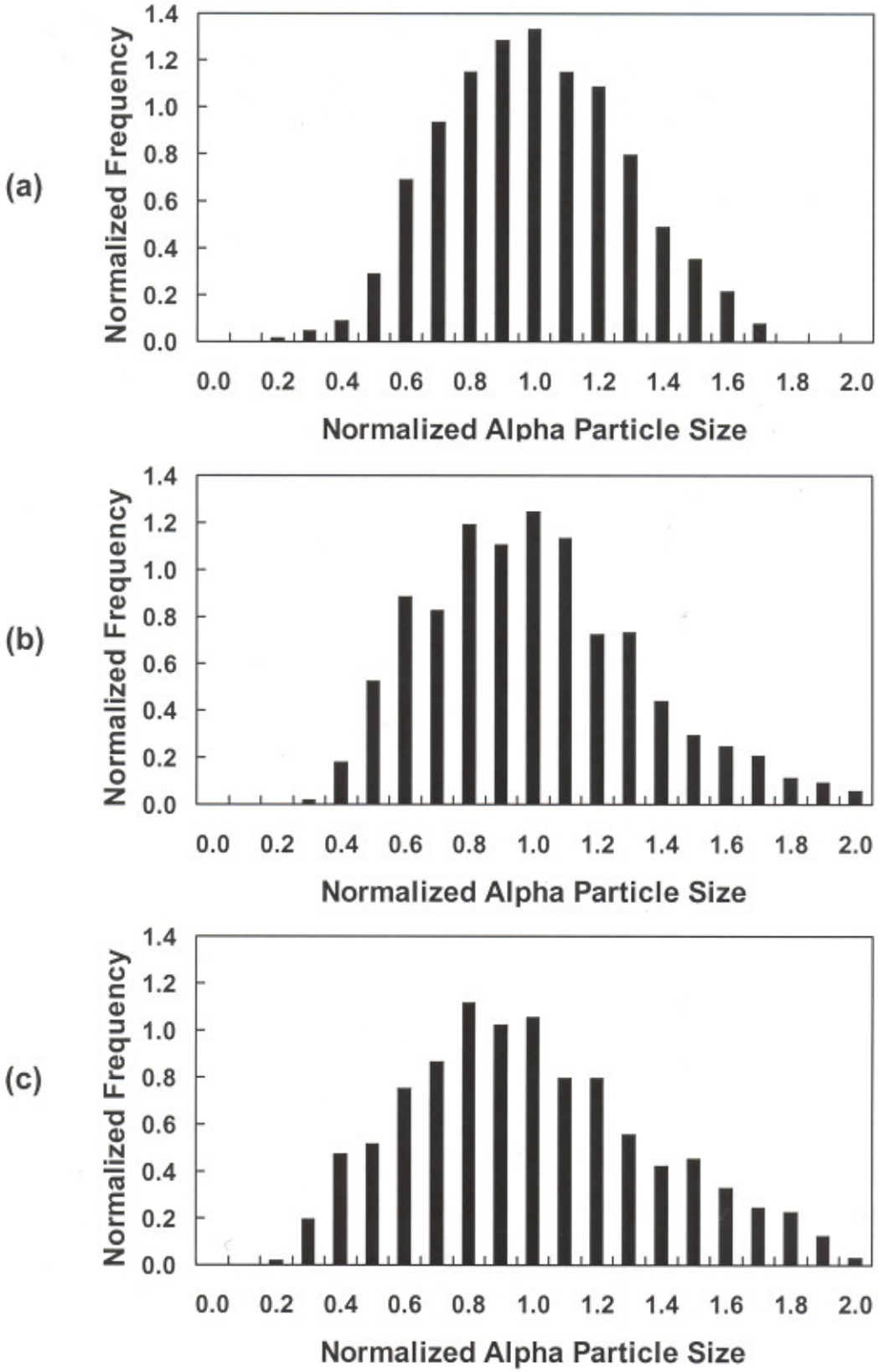

Figure 9. Particle-size distributions for UFG Ti-6Al-4V heat treated at 900°C for (a) 1h, (b) 16 h, and (c) 144 h.

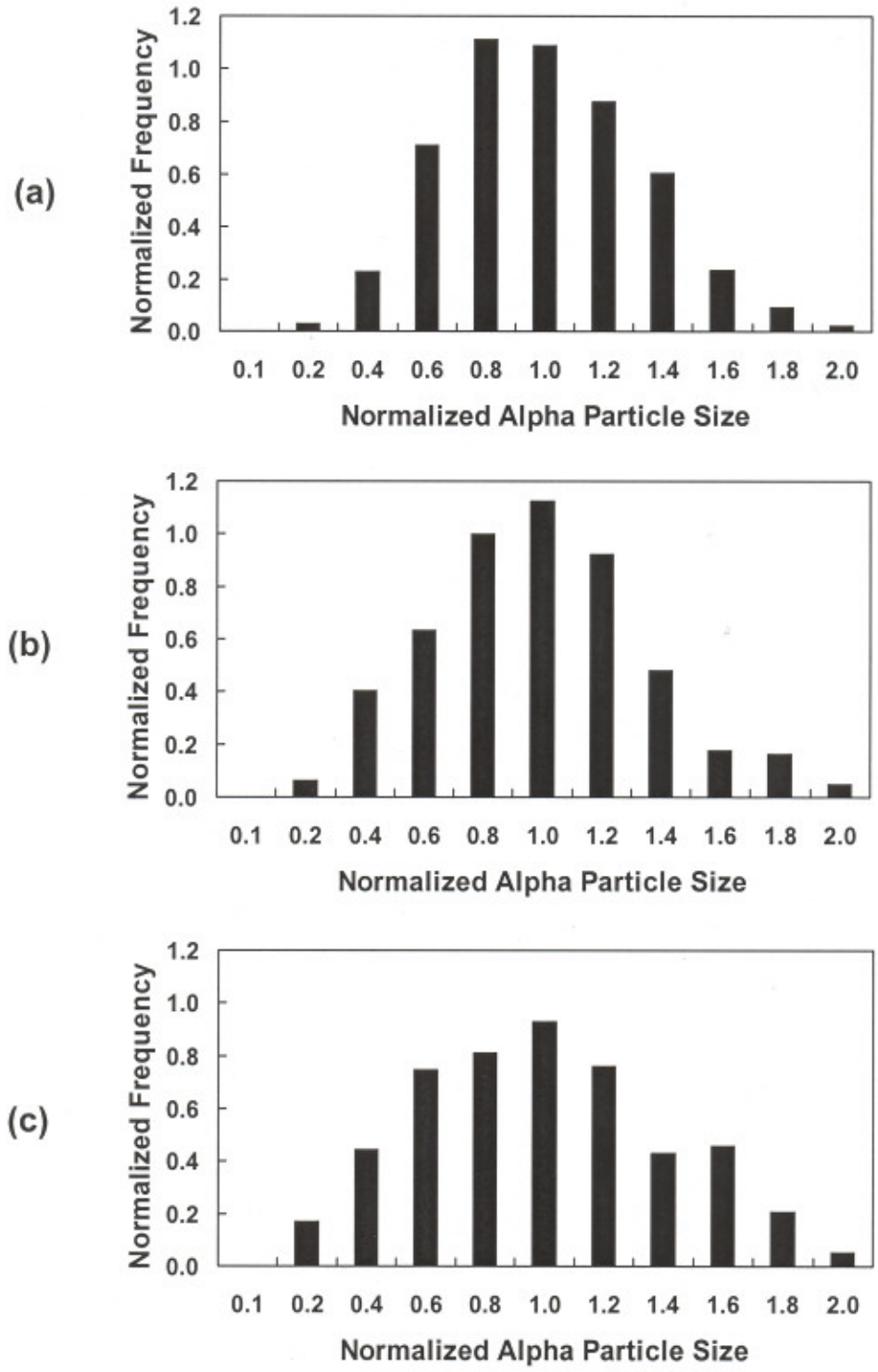

Figure 10. Particle-size distributions for UFG Ti-6Al-4V heat treated at 955°C for (a) 0.25 h, (b) 4 h, and (c) 48 h.

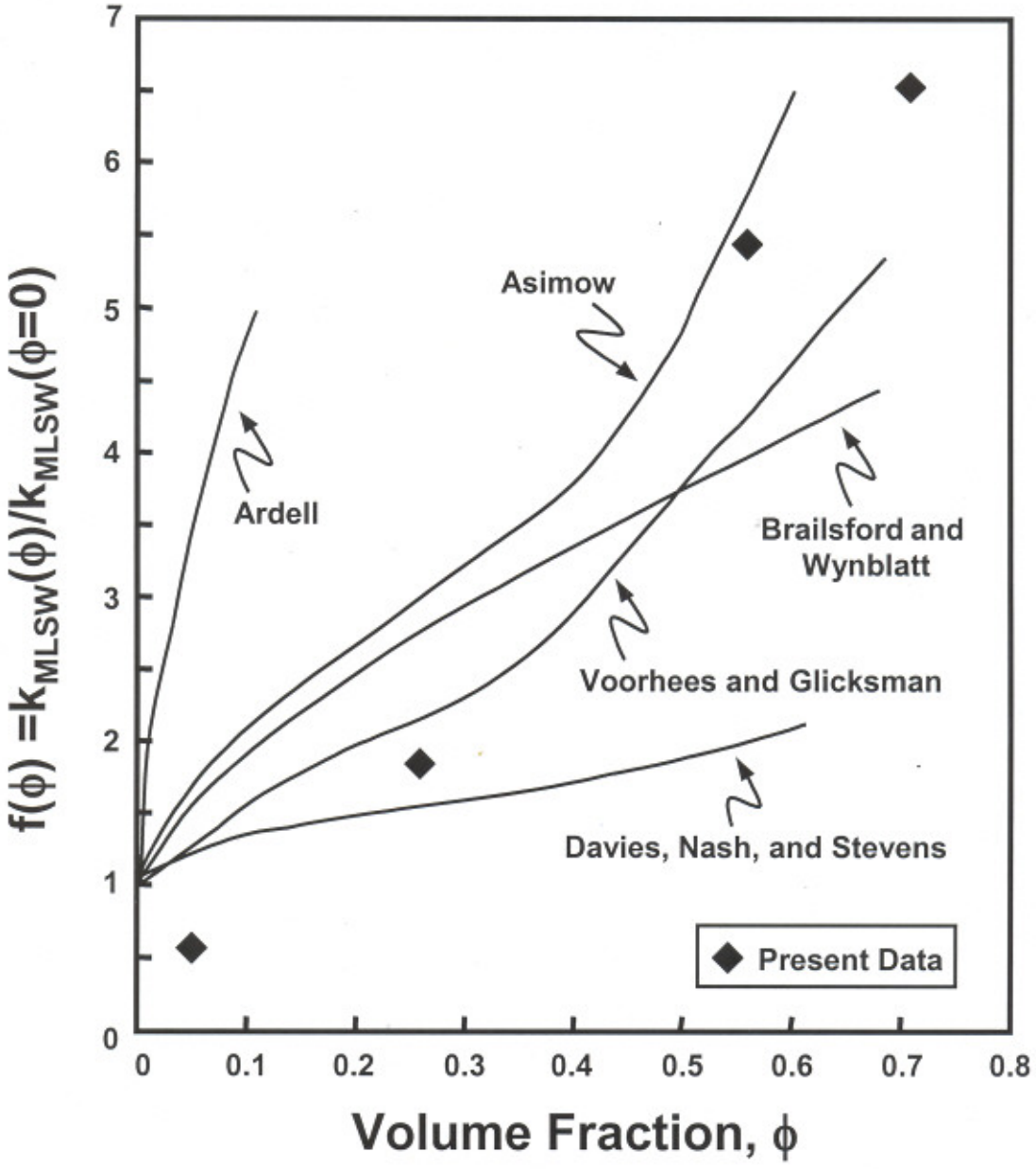

Figure 11. Comparison of model predictions of $f(\phi)$ [11] and the present results assuming $\gamma_{\alpha\beta} = 0.4$ J/m^2.